Computational Materials Science 65 (2012) 269–275

Contents lists available at SciVerse ScienceDirect

Computational Materials Science

journal homepage: www.elsevier.com/locate/commatsci

Modeling and simulation of galvanic corrosion pit as a moving boundary problem

Sunil Kumar Thamida *

Department of Chemical Engineering, National Institute of Technology, Warangal 506 004, AP, India

ARTICLE INFO

Article history:
Received 31 May 2012
Received in revised form 10 July 2012
Accepted 15 July 2012
Available online 30 August 2012

Keywords:
Anodic dissolution
Galvanic corrosion modeling
Ionic conduction
Laplace equation
Numerical simulation
Surface pore growth simulation

ABSTRACT

In this article, the dynamics of pit formation during galvanic corrosion is modeled and simulated when two dissimilar metal surfaces are in contact forming an 180° joint. As a novel advancement to the analysis of galvanic junction currents, the galvanic corrosion is mathematically modeled as a moving boundary problem represented by Laplace equation for electric potential in the electrolyte and activation driven dissolution of anode surface. In addition to numerically solving for the galvanic current density distribution, we let the anode surface dissolve and perform the calculations in the pitted surface of anode. A linear model of polarization curve or the linear resistance model is applied as the activation boundary condition at the anode and cathode surfaces. The results on progression of pit shape and current density distribution with time are presented.

1. Introduction

Galvanic corrosion usually occurs at a junction of two metals with different corrosion potentials. For example, in the galvanic series, the corrosion potential of aluminum is −0.8 V and that of magnesium is −1.6 V in a salt solution equivalent to sea water as measured against the standard calomel electrode. It suggests that a net potential difference of 0.8 V develops at a junction between magnesium and aluminum in the presence of an electrolyte or salt solution. Hence, in a composite object made of magnesium and aluminum parts, magnesium, which is on more negative side of the galvanic series, becomes anode and corrodes, while aluminum becomes a cathode and does not corrode. It is known from the experimental data that a galvanic pit develops on magnesium closer to the junction even in a very short duration, e.g. nearly at the rate of 0.5 mm per day in 1.6 wt.% NaCl solution. Such galvanic systems are shown to require specially designed experiments [1–3] in an accelerated mode in order to study long term galvanic corrosion effect and to identify methods of prevention. Galvanic corrosion effect can also be predicted from theoretical models combined with numerical simulations for various types of materials and geometries in various corrosion conditions.

Theoretical modeling of galvanic corrosion was shown to be able to predict the current density distribution around the junction causing pitting of anode only near the junction [4–6]. Corrosion software such as Beasy [7] is usually used to model the phenomenon of galvanic corrosion to optimize for cathodic protection. These models could predict the distribution of current density around a galvanic junction but not the complete dynamics of pit formation. The purpose of present numerical simulation method is to predict the shape and dynamics of a growing galvanic pit.

Galvanic corrosion involves several coupled phenomena such as electrochemical reactions, electro-migration, ionic diffusion, oxide layer formation and dissolution. For modeling purpose, only galvanic contribution to corrosion current is dealt with here to distinguish its effect in comparison to the free corrosion. Early modeling attempts have provided an analytical solution [5,6] for the galvanic current and potential distribution around a galvanic junction involving two dissimilar metals kept side by side making an 180° angle with each other and covered by a corroding solution. These theoretical predictions were also later validated with experimental measurement of the potential and current density across the junction [4]. Recently, semi-analytical and numerical methods [8–12] were developed to solve for current density distribution on anode and cathode in a galvanic couple and similar electrochemical phenomena such as electro-deposition. Simulation of pitting corrosion by cellular automaton method is also another approach [13]. Galvanic corrosion is found to be better modeled with a continuum approach than a lattice model since the curvature of the interface is an important parameter in determining the electro-chemical dissolution rate.

Simulation of the dissolving anode metal and the dynamics of galvanic pit would require solution to electrical potential governed by the Laplace equation as the anode surface is dissolving. Hence, galvanic corrosion comes under the category of moving boundary problems. A number of moving boundary phenomena such as dendrites in directional solidification [14], viscous fingers in oil–water

---

* Tel.: +91 9492079213.
E-mail address: sunil76@nitw.ac.in

0927-0256/$ - see front matter © 2012 Elsevier B.V. All rights reserved.
http://dx.doi.org/10.1016/j.commatsci.2012.07.029

Nomenclature

a	width of the anode and cathode plate, m
C_n	coefficient, dimensionless
F	faraday constant, 96,487 C/mol
j	current density, A/m^2
j_o	maximum galvanic current density, A/m^2
j^*	current density, dimensionless
k_d	electrochemical dissolution equivalence, m^3/C
M_w	molecular weight of anode metal, kg/mol
n	normal coordinate at interface, m
t	time, s
t^*	time, dimensionless
u	dissolution speed, m/s
u_o	maximum galvanic dissolution speed, m/s
w	height of electrolyte, m
x	x-coordinate, m
x^*	x-coordinate, x/a, dimensionless
z	z-coordinate, m
z^*	z-coordinate, z/a, dimensionless
α	polarization length scale, m
γ	valency of anode metal in oxidized state
ϕ	potential, V
ϕ^*	potential, dimensionless
κ	ionic conductivity, S/m
λ_n	eigenvalue, dimensionless
θ_n	angle between normal to pit interface and $-$ve z-axis, rad
τ_o	time scale, s

Subscripts

a	anode
c	cathode
o	open circuit potential

Hele-Shaw type of flows [14] and nanopores in anodic alumina [15] are a few examples of interfacial patterns resulting from propagation of one medium into another or by phase transformation or by surface dissolution. Galvanic corrosion is similar to the electro-deposition phenomena in reverse where the shape changes occur on cathode during electro-deposition while shape changes occur on anode during galvanic corrosion. A number of modeling and simulation approaches [10–12] are used to solve the electro-deposition kinetics by a moving boundary approach and these methods could be applied to galvanic corrosion also. In electro-deposition a semi-analytical method [10], level set method [11], and Euler method [12] are developed to obtain solution to the dynamics of the cathode surface or the deposited film in a trench as a function of time. The galvanic pit dynamics on the other hand resembles a half-pore growing into the anode metal.

2. Modeling approach

Two dissimilar metals could be joined making 180 ° Contact angle with each other, as shown in Fig. 1. Such geometry does not include far field effects as in the case of other geometries of joints. But theoretically, the numerical solution near the junction is more important than the far field effects in estimating the concentration of galvanic corrosion current. The metals are supposed to be of equal width 0.5a represented as 0.5 in Fig. 1 after normalizing with a as the length scale. The metals are covered with an electrolyte up to a thickness of w and represented as w/a in Fig. 1. The top surface of the electrolyte can be modeled as a no-flux condition since air acts as an insulator. The left and right sides display a symmetry or no-flux condition.

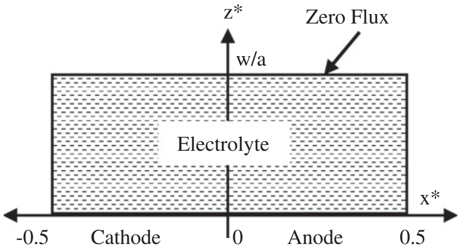

Fig. 1. Schematic diagram of the galvanic junction in contact with electrolyte used for mathematical modeling.

Electrochemically, galvanic corrosion is equivalent to two metals at different corrosion potentials kept in contact with each other in a conducting solution, e.g., 1.6 wt.% NaCl dissolved in distilled water. Because of the potential difference, there would be an electric field directed from anode towards cathode in a semi circular path. This would become clear when the exact solution to Laplace equation is obtained as described in the following sections. There would be a gradual variation of the magnitude of electric field along the metal surface with highest electric field near the junction and gradually decaying with distance from junction. The electric field causes ions to move in the solution to maintain current between anode and cathode. If magnesium is the anode, an electrochemical reaction occurs as $Mg \rightarrow Mg^{2+} + 2e^-$ liberating Mg^{2+} ions into the electrolyte forming a complex or precipitate with Cl^- ions while electrons pass from anode to cathode on the metal side. At cathode, or aluminum in this example, H^+ ions form H_2 gas by receiving electrons from aluminum which are supplied by magnesium metal. During this process, there is ion transport and redistribution of Mg^{2+}, H^+, Cl^- and Na^+ in the electrolyte in order to maintain electro neutrality. The driving force for this transport is electric field which is the gradient of potential. The electrical potential in the electrolyte is governed by electrostatics described by Poisson equation which reduces to Laplace equation Eq. (1) with electro-neutrality assumption.

$$\nabla^2 \phi = 0 \tag{1}$$

It is also assumed that the electrolyte is continuously stirred and hence the concentration of the ions is uniform though there is equal and opposite flux of oppositely charged ions. In the case of transport-limited transients, the phenomena could be well modeled by a complete set of electro-migration and diffusion equations [16].

Modeling and specifying the boundary conditions for potential at the anode and cathode surfaces is the most crucial part of the problem and will require some valid assumptions. A first choice is that the potential of each surface is approximately the same as their free corrosion potential, $\phi_{o,a}$ for anode and $\phi_{o,c}$ for cathode which is -1.6 V for Mg and -0.8 V for Al. But this is true only under zero current condition. As the current begins to flow, the potential at the metal surface has to increase or decrease depending on the sign, which can be obtained from the polarization curve of the metal in that electrolyte medium. For the purpose of modeling, we first assume a linear polarization curve with constant slope as

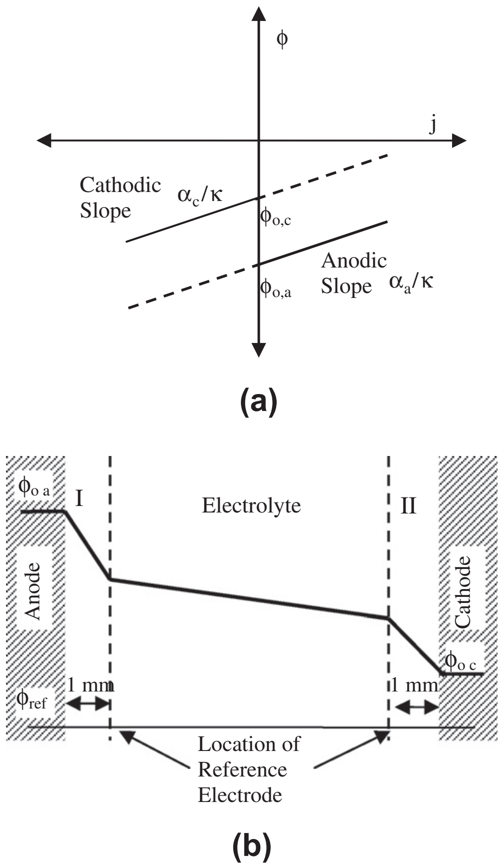

Fig. 2. (a) Schematic diagram of linear approximation of polarization curves of two dissimilar metals. (b) Schematic diagram of potential variation between two dissimilar metals in the electrolyte. Regions I and II are the polarized layers and the zone in between is the Ohmic region.

shown schematically in Fig. 2a for a hypothetical anode and cathode pair. Beyond a certain applied potential, there will be acceleration of anodic current, then oxide formation and passivation events resulting in a relatively constant corrosion current with no major increase until the oxide layer breaks down. This is usually modeled using Tafel curves or Butler–Volmer expression with two exponential terms representing the relationship between the over potential and current density [17].

There are other phenomena such as electrokinetic flow where linear polarization model is applied [18,19]. Latest studies show that the linearized model is invalid for high polarization [20,21]. In Galvanic corrosion, the potential difference between the metal surfaces is only of the order of 1 V since the open circuit potentials of most metals are not far apart in common electrolytes such as NaCl solution in water. There could be situations with large potential difference where the nonlinear polarization model may have to be applied. Hence the present analysis with linear model would hold good for galvanic pairs with small potential difference and probably for micro galvanic corrosion too.

Solving the Laplace equation with such nonlinear boundary conditions is not possible using boundary element method or the linear solvers using finite element method which formulate a linear matrix equation for computing the solution. These numerical solvers require the boundary condition to be in the form of current density being linearly proportional to the over potential. To take into consideration the features of polarization such as exponential dependence of current density with over-potential and passivity, it needs a robust numerical method which can take input boundary conditions as a tabulated data. There is currently available technical computation software like COMSOL which can solve Laplace equation for tabulated boundary condition. In this paper, we present the simulation results for pit dynamics based on a linear approximation of the polarization boundary condition.

For the sake of understanding the role of various key parameters, we choose a linear form of the polarization curve. Solving the galvanic corrosion problem with actual polarization curve or the exponential form of Tafel curve as boundary condition is not attempted in the present work but will be explored as a future extension. Analytical methods are possible for linear mixed boundary conditions and rectangular or circular geometries. Hence, linear polarization model is usually employed to obtain a qualitative solution for planar [5] and circular geometry [6].

In the linear form, the over potential, which is the difference between metal potential and reference electrode potential ($\phi - \phi_o$), is approximated to be proportional to surface current density j or dissolution rate as described in Eq. (2) and represented schematically in Fig. 2a. Eq. (2) is a generic polarization equation for a metal and the two slopes in Fig. 2a are to represent the dissimilarity of anode and cathode metals in any given galvanic junction.

$$\phi = \phi_o + \frac{\alpha}{\kappa} j \tag{2}$$

The proportionality constant or slope is represented as α/κ where α is the polarization length scale (meters) of the metal, e.g. α_a for anode and α_c for cathode and κ is the conductivity (Siemens/meter) of the electrolyte. The slope α/κ is also referred to as the linear polarization resistance of a metal. This polarization relationship of current versus over potential becomes the lumped boundary condition applied at the location of reference electrode plane instead of the metal surface as shown in Fig. 2b. So, we would be solving for the electric potential distribution in the Ohmic electrolyte zone between the metals excluding the micron-thick polarized layers shown as I and II. Such a simplification helps to overcome the difficulty of solving the Debye layer electrochemistry. Also the experimental data from polarization curve could be utilized as the boundary condition. During galvanic corrosion, the current density j varies from point to point on the surface. Hence, local activation potential on the metal is also a function of the local current density giving rise to a mixed boundary condition, which is a combination of Dirichlet and Neumann condition. Further, another approximation, as shown in Eq. (3), that the ionic current density j in the electrolyte is proportional to the local normal electric field $\partial\varphi/\partial n$ into the metal, is also applied to proceed further in solving the problem.

$$j = -\kappa \frac{\partial \phi}{\partial n} \tag{3}$$

Such an approximation holds good when there is no concentration variation of the salt in electrolyte. Therefore, the linear mixed boundary condition in Eq. (2) combined with Eq. (3) is now simplified to Eq. (4) which is a regular mixed Neumann boundary condition.

$$\phi = \phi_o - \alpha \frac{\partial \phi}{\partial n} \tag{4}$$

Some of the implicit assumptions included in this approach are: (a) there is no stagnation effect of ions, (b) no concentration variation of the corroding solute and (c) no oxide layer builds up at anode or cathode that alters the polarization curve.

Let the plates be of equal width 0.5a each. By taking the width ‘a’ as the length scale, Eq. (4) can be non-dimensionalized to give Eqs. (5a) and (5b).

$$\text{At anode,} \quad \phi^* = 1 - \frac{\alpha_a}{a} \frac{\partial \phi^*}{\partial n^*} \tag{5a}$$

$$\text{At anode,}\quad \phi^* = -\frac{\alpha_c}{a}\frac{\partial \phi^*}{\partial n^*} \tag{5b}$$

where $\phi^* = (\phi - \phi_{o,c})/(\phi_{o,a} - \phi_{o,c})$ is the dimensionless form of potential, $\phi_{o,a}$ is the anodic corrosion potential, $\phi_{o,c}$ is the cathode corrosion potential, 'α_a' is the polarization length scale of anode and 'α_c' is the polarization length scale of cathode. 'a' is the length scale of the metal extent. Potential is also appropriately scaled with difference in galvanic voltages of cathode and anode after referencing cathode potential as zero. The boundary conditions Eqs. (5a) and (5b) are similar for anode and cathode except that there is a step change in base potential. Mathematically the step function is $H(x^*) = 1$ for $x^* > 0$ (anode) and $H(x^*) = 0$ for $x^* < 0$ (cathode). It is to be noted that, we obtain a variable parameter 'α_a/a' for anode and 'α_c/a' for cathode metal as in Eq. (5a) which is the ratio of polarization length scale to metal domain size. Similarly, we obtain a physical parameter j_o in Eq. (6b) which is the maximum current density that would result when the maximum potential difference of anode and cathode is applied to anode.

$$j^* = \frac{j}{j_o} = -\frac{\alpha}{a}\left(\frac{\partial \phi^*}{\partial n^*}\right) \tag{6a}$$

$$j_o = \frac{\kappa}{\alpha_a}(\phi_{o,a} - \phi_{o,c}) \tag{6b}$$

The material dissolution speed is usually given by the product of current density and electrochemical dissolution equivalence constant of the metal as in the following equation:

$$u = \kappa_d j \tag{7}$$

Here u is the dissolution speed and k_d is given by $M_w/(\rho\gamma F)$ where M_w is the molecular weight of the anodic metal, γ is the valency of anode metal in oxidized state, ρ is metal density and F is the Faraday constant.

A time scale τ_o is defined as in Eq. (8) and it approximately represents the time required for galvanic corrosion to spread from the junction to a depth equal to the polarization length scale of the anode metal under extreme possible galvanic condition.

$$\tau_o = \frac{\alpha_a}{u_o} \tag{8}$$

Here, u_o is the maximum dissolution speed given by

$$u_o = \kappa_d \frac{\kappa}{\alpha_a}(\phi_{o,a} - \phi_{o,c}) \tag{9}$$

Local dissolution speed of the interface in dimensionless form is proportional to the local azimuthal component of current density j^* in z^* and x^* directions as shown schematically in Fig. 3. The vertical and horizontal components of this dissolution speed are defined in Eqs. (10a) and (10b) where θ_n is the angle made by the normal to pit surface with vertical direction such that $\tan\theta_n = dz/dx$ locally as in Fig. 3.

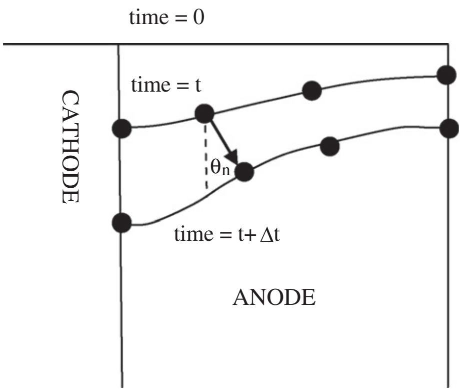

Fig. 3. Update scheme for the nodes on the moving boundary of anode surface during galvanic corrosion simulation.

$$\frac{dz^*}{dt^*} = -\frac{\alpha_a}{a} j^* \cos\theta_n^* \tag{10a}$$

$$\frac{dx^*}{dt^*} = -\frac{\alpha_a}{a} j^* \sin\theta_n^* \tag{10b}$$

$$t^* = \frac{t}{\tau_o} \tag{11}$$

Here t^* is the dimensionless form of time. It is interesting to note that we have finally three variable parameters: 'α_a/a' and 'α_c/a' in the boundary condition in Eqs. (5a) and (5b) and a parameter 'w/a' for the geometry as in Fig. 1. Hence, only these parameters need to be varied to simulate galvanic corrosion for various possible electrolyte conditions and metals bearing a linear polarization curve. The possible deviations from these idealized conditions are that the polarization curve can be nonlinear for various metal-electrolyte combinations. With the above simplification, the problem reduces to solving the Laplace equation in Eq. (1) with linear mixed boundary condition as in Eqs. (5a) and (5b) for the pit geometry of Fig. 1. Solution for the rectangular geometry of Fig. 1 is already shown to be possible by spectral expansion analytically [5] for $\alpha_a = \alpha_c = \alpha$ as given in the following equation:

$$\phi^*(x^*, z^*) = 0.5 + \sum_{n=1}^{\infty} C_n \cos h\lambda_n\left(\frac{w}{a} - z^*\right)\sin\lambda_n x^* \tag{12}$$

where $x^* = x/a$, $z^* = z/a$, the coefficients are

$$C_n = 2/\lambda_n[\cosh(\lambda_n w/a) + \alpha/a)\lambda_n \sinh(\lambda_n w/a)]$$

And eigenvalues are $\lambda_n = (2n - 1)\pi$.

As the metal dissolves or corrodes, the surface forms a pit as in Fig. 3. and it no longer remains rectangular and analytical solution for this dynamically changing geometry is difficult unless by a suitable conformal mapping method. On the other hand, numerical solution can be used in any irregular geometry with suitable boundary conditions. Some of the numerical methods for solving Laplace equation are finite difference method (FDM) [8], boundary element method (BEM) [3,9] and finite element method (FEM). In this work, we use the numerical solver PDETOOL of MATLAB [23], which employs the FEM method.

3. Simulation results

Simulation results are obtained for various values of the non-dimensional parameters in the problem: (a) ratio of polarization length scale to metal surface size kept at $\alpha_a/a = \{0.5, 0.1, 0.05, \text{and } 0.01\}$ and (b) ratio of polarization length scales of anode and cathode, $\alpha_a/\alpha_c = \{1, 0.5, 0.1, \text{and } 0.01\}$. It is already known that, for electrolyte thickness of '$w/a > 0.5$', the solution approaches almost the same result as that for infinite thickness of electrolyte [5]. Hence numerical solutions were obtained with '$w/a = 0.5$' that is for the most severe corrosion condition of large electrolyte coverage. First, the present numerical tool is verified to be accurate since the numerical solution for potential and current density distribution on the electrode surfaces $z^* = 0$ at zero time matches with the analytical solution of Eq. (12) as shown for certain parameter set in Fig. 4a and b.

As shown in Fig. 3, the anode surface is allowed to dissolve or corrode. In this process a pit or trench forms which becomes wider and deeper with time as shown from simulation. The pit region also gets filled with the electrolyte in reality and hence we need to solve the Laplace equation in this new geometry. The junction

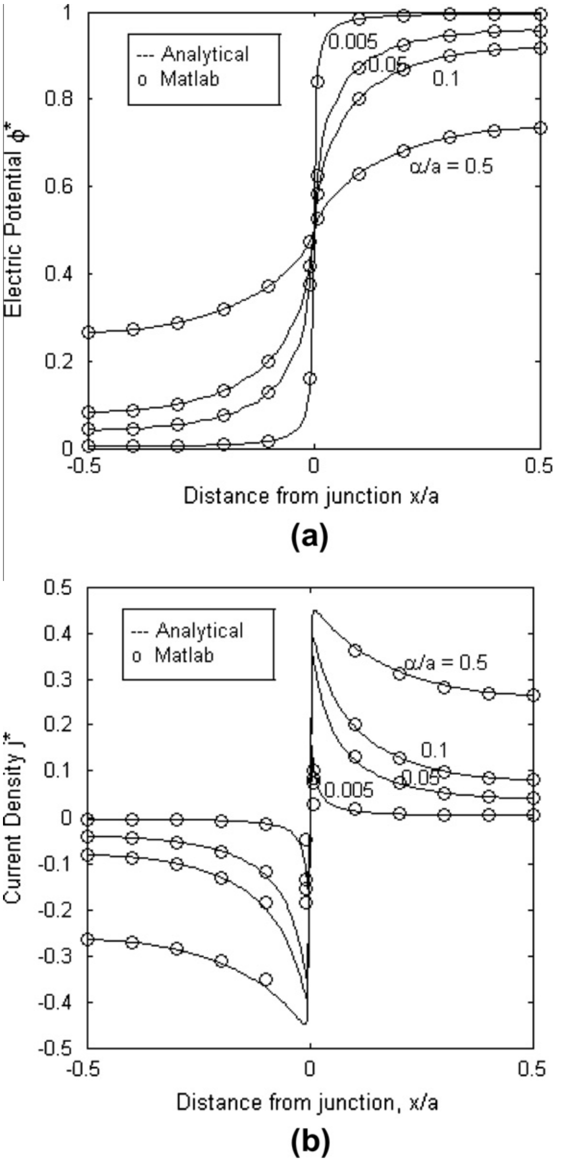

Fig. 4. Present numerical solution using PDETOOL of MATLAB is obtained and compared with analytical solution Eq. (12) at time zero for parameters $w/a = 0.5$, $\alpha_a/\alpha_c = 1$ and $\alpha_a/a = \{0.5, 0.1, 0.05 \text{ and } 0.005\}$ as shown in (a) for potential distribution and (b) for current density distribution.

point of anode with cathode is assumed to slide down along the cathode surface. Hence the pit would have cathode surface exposed as it propagates into the anode metal. In numerical simulation, the moving boundary of anode is segmented into 50 divisions with dx^* of 0.01 α_a/a in dimensionless units in order to allow flexibility for dissolving and be able to simulate the accurate pit morphology. A small number of segments would lead to sharp corners and abrupt variation in curvature at the nodes which may not give the accurate variation of the surface contour. On the other hand, a large number of segments would cause overlapping of nodes in subsequent time steps and lead to numerical errors and insolvable geometry. Ideally, in problems involving pore formation and the like, an adaptive segmentation is used, where the local boundary segment length is taken to be equal to a fraction (ex: 1/10th) of the local radius of curvature at every time step [14]. In the present case, only one pit is formed and it does not contain the feature of undulations, hence a reasonably small segment length is taken and it is found to display a smooth variation of the anodic surface while it is dissolving. Another way to arrive at the optimum number of segments is to minimize the standard deviation between the surface profiles obtained at the end of certain simulation time. Each node on the anode surface is moved downwards into the metal after every time step with the components of dissolution speed given by Eqs. (10a) and (10b). Near the junction, as anode dissolves, new surface of the cathode is exposed to electrolyte. This process of simulation is repeated over several time steps and the shape of pit at various times is plotted.

3.1. Effect of polarization length scale, α_a/a

In the first case, we simulated the pit to see the effect of area or width of anode and cathode in comparison to the polarization length scale. Other parameters are kept constant as cathode to anode area ratio equal to 1 and ratio of polarization coefficients $\alpha_a/\alpha_c = 1$. For this purpose α_a/a is varied from 0.5 to 0.01. Larger α_a/a corresponds to micro galvanic corrosion and smaller α_a/a corresponds to macro galvanic corrosion. The polarization length scale of anode and cathode are kept equal. The pit shape dynamics are plotted for one particular parameter in the mid range $\alpha_a/a = 0.05$ in Fig. 5a. The pit bottom near the junction moves faster than rest of the interface. The length units are rescaled with α_a as the unit of measure to appropriately represent the simulation results of pit growth as the width of the plates increases. The current density distribution along anode and depth of the pit bottom as a function of time are plotted in Fig. 5b and c. The pit is in the form of a triangular trench as seen in Fig. 5a. The current density is highest at the junction and increases in nearby locations with time. For large α_a/a, as the simulation time progresses, the pit widens to cover the width of anode and begins to propagate downward. Comparison of simulated pit shape in Fig. 5a with experimental images would show that the simulation is comparable to real phenomena.

Experimental images would also indicate that the galvanic pitting is limited to only certain distance from the cathode–anode junction and simulation too predicts the same. The distribution of current density on the anode surface with time in Fig. 5b shows that the current density near the junction point of anode and cathode or the pit bottom is constant at 0.5 in dimensionless units. But away from the junction, the current density increases by a fraction with time. The reasons for this are: (1) With time, the anode surface changes to a curve instead of being flat. Though an increase in the magnitude of current density is seen in Fig. 5b, to compute the vertical dissolution speed, we need only the fractional $\cos\theta_\mathrm{n}$ component of the total normal dissolution speed as depicted schematically in Fig. 3. Similarly, the horizontal component of the dissolution speed is computed from $\sin\theta_\mathrm{n}$ fraction of the total normal dissolution speed. Hence, it appears in Fig. 5a that the pit contour moves downwards into the anode surface at nearly a constant speed. (2) At the junction or bottom tip point, the pit surface remains horizontal locally implying that $\theta_n = 0°$ or $\cos\theta_\mathrm{n} = 1$ at a maximum value. In addition to this, the magnitude of current density on the anode is maximum near the junction due to proximity to cathode. Hence, the vertical speed at the pit bottom is maximum and constant at a value of 0.5 in dimensionless units as a function of time as shown in Fig. 5c.

Simulation indicates that the depth of the pit as seen in Fig. 5c increases at a constant speed of $0.5u_o$ which is the maximum possible galvanic dissolution speed possible as discussed in earlier section. Hence the depth of the pit after a certain time 't' can be predicted as $0.5u_ot$ or $0.5(t/\tau_o)\alpha_a$ and the width of the prominent portion of the pit is approximately equal to the depth of the pit. In many other phenomena as well, the interface forms pore like structures propagating at maximum possible speed also known as maximum velocity principle (MVP) [14].

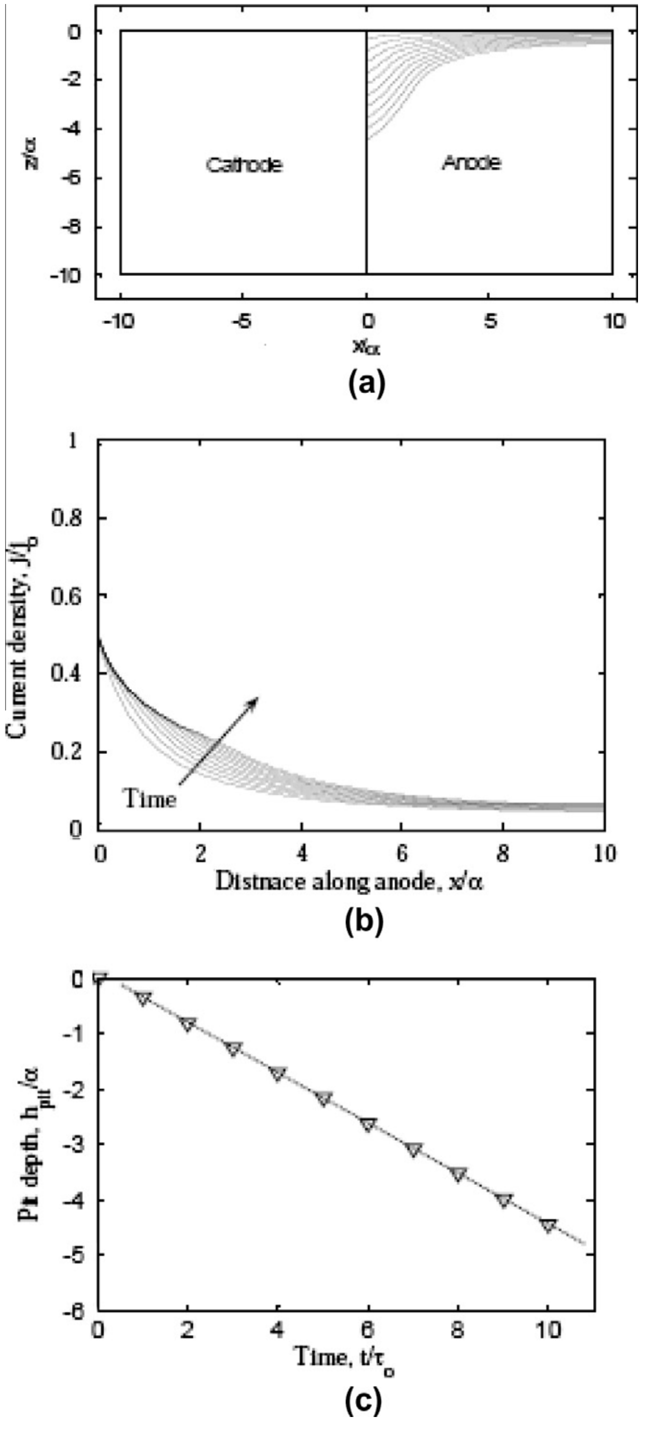

Fig. 5. Simulation results for parameters $\alpha_a/a = 0.05$, $\alpha_a = \alpha_c = \alpha$ and $w/a = 0.5$. (a) Pit shape in the galvanically corroding anode metal as a function of time plotted after every time interval of τ_o for 10 such time periods. (b) Current density across the anode pit surface. (c) Depth of the pit at junction as a function of time.

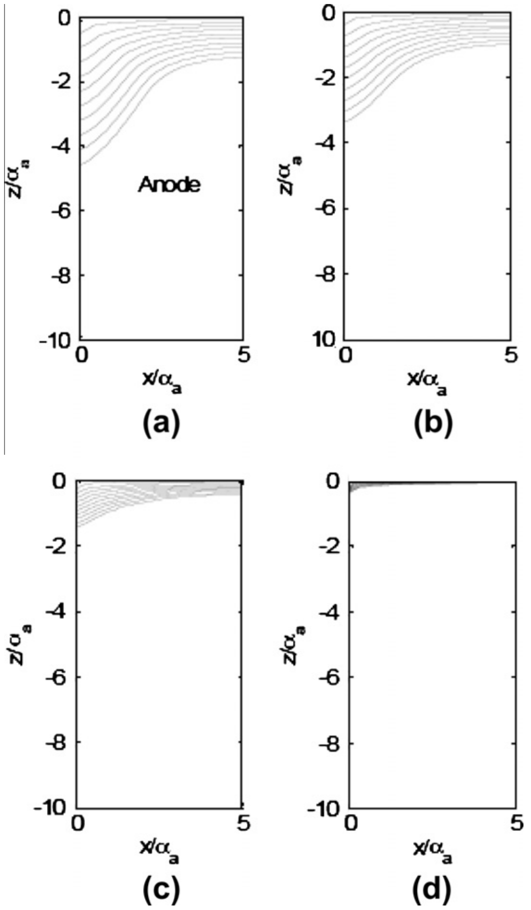

Fig. 6. Pit shape in the galvanically corroding anode metal as a function of time as obtained from simulation with $\alpha_a/a = 0.1$' and '$w/a = 0.5$'. α_a/α_c is varied as (a) 1, (b) 0.5, (c) 0.1 and (d) 0.01.

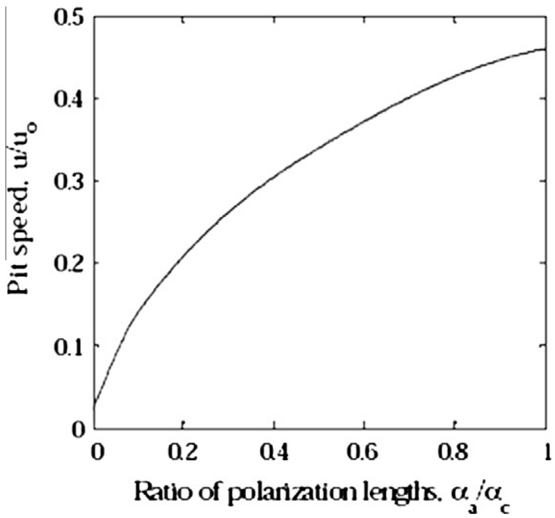

Fig. 7. Speed of pit propagation as obtained from simulation for various values of ratio of polarization length scale α_a/α_c.

3.2. Effect of unequal polarization lengths α_a/α_c = {1, 0.5, 0.1 0.01}

The cathodic currents of aluminum are an order of magnitude less than the anodic currents of magnesium unlike what is indicated by the polarization curves in Fig. 2a. Practically, it would mean that the area ratio of cathode to anode becomes an influencing factor as in the case of magnesium and aluminum whose ratio of polarization coefficients is around 0.01. Such a condition of dissimilar polarization coefficients if incorporated in the model would predict the galvanic corrosion accurately and closer to as seen experimentally in Fig. 1. In Fig. 2a if the slope of anode is kept constant and the slope of the cathode is changed by making it steeper, it implies higher polarization resistance of cathode or higher value of α_c. The ratio α_a/α_c would then become the parameter of interest.

By keeping rest of the parameters constant as cathode to anode area ratio = 1, $w/a = 0.5$ and $\alpha_a/a = 0.1$, we varied α_a/α_c as $\{1, 0.5, 0.1, 0.01\}$.

The results of the simulated pit shape versus time are plotted in Fig. 6a–d. It is observed that the extent and depth of the pit becomes smaller as α_a/α_c decreases. The speed of pit remains more or less constant during each simulation though the magnitude is different. Hence, a measure of average pit speed u/u_o is plotted against α_a/α_c in Fig. 7. It can be seen that the pit speed decreases as the polarization resistance of cathode increases.

4. Conclusions

The simulation results can be used as a correlation tool to predict galvanic pitting for various metal combinations and electrolyte conditions. For instance, the experimental galvanic pit is comparable to the simulated pit shapes of Fig. 5a. These simulation results help in providing a better understanding of the galvanic corrosion phenomenon and insights about pit depth and width variation with time for engineering applications in the area of durability based design. Under a corroding environment, similar pits could be propagating in the anodic portion of an alloy leading to micro galvanic corrosion. The model can be potentially extended to study micro galvanic action at the microstructural scale as well. The model has linear polarization curves as the basis, but is idealized for mathematical convenience.

Though we have assumed that there would not be any hydrodynamic effect on ion accumulation in the electrolyte, it could be possible for micro vortex generation due to induced polarization as discovered in electrokinetic flows [21,22]. If we examine the galvanic corrosion results as shown in Fig. 4b, the surface current or the normal electric field is non-zero and changes its sign near the metallic junction. Hence there would be an induced zeta potential of opposite signs as well. There would also be a tangential electric field directed from anode towards cathode as can be inferred from potential variation as shown in Fig. 4a. The combination of oppositely charged zeta potential and tangential electric field would try to cause oppositely directed nonlinear Smoluchowski slip velocities at the junction [22]. But the intensity of these slip velocities would be very small since the generated normal electric field is very small and of the order of ratio of potential difference of the metals to their polarization length scale. Hence there may not be vortex generation in galvanic junction unlike the other phenomena of electrokinetic flow where singularity of electric field causes micro vortices.

With improved simulation techniques incorporating the actual polarization data of a given metal in a particular corroding environment, it is possible to simulate the galvanic corrosion phenomena more accurately. By taking the moving boundary approach, we demonstrate that the resultant shape of the pit is strikingly similar to experimental images. It is possible to simulate long term durability of galvanic joints for a wide range of parameters such as difference in galvanic potentials of metals, ratio of their linear polarization resistances, cathode to anode area ratio and electrolyte thickness.

References

[1] G. Song, B. Johannesson, S. Hapugoda, D. John, Corros. Sci. 46 (2004) 955–977.
[2] J.X. Jia, A. Atrens, G. Song, T.H. Muster, Mater. Corros. 56 (2005) 468–475.
[3] J.X. Jia, G. Song, A. Atrens, Mater. Corros. 56 (2005) 259–270.
[4] H.R. Copson, J. Electrochem. Soc. 84 (1943) 71–80.
[5] J.T. Waber, B. Fagan, J. Electrochem. Soc. 103 (1956) 64–72.
[6] E. Mccafferty, J. Electrochem. Soc. 124 (1977) 1869–1878.
[7] BEASY Corrosion and Cathodic Protection Software. For product information visit. <www.beasy.com>.
[8] P. Doig, P.E.J. Flewitt, J. Electrochem. Soc.: Electrochem. Sci. Technol. 126 (1979) 2057–2063.
[9] S. Aoki, K. Kishimoto, Math. Comput. Model. 15 (1991) 11–22.
[10] V.R. Subramanian, R.E. White, J. Electrochem. Soc. 149 (2002) 498–505.
[11] D. Wheeler, D. Josell, T.P. Moffat, J. Electrochem. Soc. 150 (2003) 302–310.
[12] A.C. West, S. Mayer, J. Reid, Electrochem. Solid-State Lett. 4 (2001) 50–53.
[13] B. Malki, B. Baroux, Corros. Sci. 47 (2005) 171–182.
[14] P. Pelce, Dynamics of Curved Fronts, Academic Press, New York, 1988.
[15] S.K. Thamida, H.C. Chang, Chaos 12 (2002) 240–251.
[16] V. Botte, D. Mansutti, A. Pascarelli, Appl. Numer. Math. 55 (2005) 253–263.
[17] D.A. Jones, Principles and Prevention of Corrosion, second ed., Macmillan, New York, 1996.
[18] Y. Ben, H.C. Chang, J. Fluid mech. 461 (2002) 229–238.
[19] Hsueh.-Chia. Chang, Leslie.Y. Yeo, Electrokinetically Driven Microfluidics and Nanofluidics, Cambridge University Press, New York, 2010.
[20] G. Yossifon, P. Mushenheim, Y.C. Chang, H.C. Chang, Phys. Rev. E 7 (9) (2009) 046305.
[21] G. Yossifon, H.C. Chang, Phys. Rev. Lett. 10 (1) (2008) 254501.
[22] S.K. Thamida, H.C. Chang, Phys. Fluids 14 (2002) 4315–4328.
[23] We use MATLAB version 7.0.1, The Mathworks Inc. For product information visit. <www.mathworks.com>.